*Desalination and Water Treatment*
www.deswater.com

doi: 10.1080/19443994.2016.1148641

57 (2016) 29411–29420
December

Taylor & Francis
Taylor & Francis Group

# Sulfate radicals from $Fe^{3+}$/persulfate system for Rhodamine B degradation

Yongsheng Lu, Xingxing Yang, Lu Xu, Zhan Wang, Yunfeng Xu*, Guangren Qian

*School of Environmental and Chemical Engineering, Shanghai University, No. 99 Shangda Rd., Shanghai, 200444, P.R. China, Tel. +86 21 66137748; Fax: +86 21 66137761; emails: luys7174@shu.edu.cn (Y. Lu), yangziyangxing@163.com (X. Yang), xulu_deer@163.com (L. Xu), wangzhan0315@163.com (Z. Wang), Tel. +86 21 66137745; Fax: +86 21 66137761; email: yfxu@shu.edu.cn (Y. Xu), Tel./Fax: +86 21 66137758; email: grqian@shu.edu.cn (G. Qian)*

Received 25 November 2015; Accepted 26 January 2016

## ABSTRACT

The $Fe^{3+}$/persulfate system for Rhodamine B (RhB) oxidative degradation has been investigated. The catalytic mechanism in the $Fe^{3+}$/persulfate system was proposed as follows: $Fe^{3+}$ was restored to $Fe^{2+}$ by the generated intermediate products during the degradation process. The influence parameters were examined in batch experiments, including $Fe^{3+}$ and persulfate concentration and initial pH. The results indicated that the $Fe^{3+}$/persulfate system exhibited good performance for RhB degradation and followed first-order kinetics. 95.91% of the RhB was removed within 30 min under the following conditions: $[Fe^{3+}]_0 = 1$ mM, $[\text{persulfate}]_0 = 1$ mM and pH 3.0. The RhB degradation efficiencies increased as the $Fe^{3+}$ and persulfate concentrations increased. In addition, the RhB degradation was inhibited in the presence of inorganic anions, which was primarily due to a complex reaction between $Fe^{3+}$ and various anions except for $NO_3^-$.

*Keywords:* Persulfate; $Fe^{3+}/Fe^{2+}$; Sulfate radicals; Degradation

## 1. Introduction

Advanced oxidation processes (AOPs) that are based on radicals with high oxidization abilities, have been developed for the treatment of wastewater containing organic contaminants [1,2]. $H_2O_2$ activated by several $Fe^{2+}$ containing catalysts produces hydroxyl radical ($^{\cdot}OH$), and these reagents are known as Fenton and Fenton-like reagents and widely applied [3,4]. However, these reagents exhibit limitations, such as the rigorous pH required for Fenton reagent and the low stability of $H_2O_2$. Recently, SR-AOPs based on sulfate radicals ($SO_4^{\cdot-}$) have emerged as an approach for organic pollutant degradation. In comparison to $^{\cdot}OH$, the sulfate radical ($SO_4^{\cdot-}$) is more selective for oxidation at neutral pH with a similar oxidation ability [5,6].

Persulfate (PS, $S_2O_8^{2-}$) oxidation has been employed for the degradation of various contaminants that can form sulfate radicals through photochemical [7], thermal [8], sono [9], magnetic spinel [10], zero valent iron [11], bimetallics and trimetallics [12], iron waste [13], or transition metal [14] methods. Among these methods, transition metal-based activation (i.e. $Co^{2+}$, $Fe^{2+}$, $Ag^+$, $Ru^{3+}$, and $Cu^{2+}$) has been commonly used as an efficient method for the generation of

---

*Corresponding author.

*Presented at the 8th International Conference on Challenges in Environmental Science & Engineering (CESE-2015)*
*28 September–2 October 2015, Sydney, Australia*

sulfate radicals. Due to cost savings, as well as the risks of using heavy metals to human health and the environment, environmentally friendly ferrous iron ($Fe^{2+}$) has received increasing attention for the activation of PS to generate sulfate radicals (Eq. (1)). Nevertheless, this activation approach has its intrinsic drawback because excess $Fe^{2+}$ in $Fe^{2+}$/PS system could consume the produced sulfate radicals (Eq. (2)) [15]. By considering the reaction stoichiometric efficiency [16], the lower degradation efficiency is obtained when the sulfate radical concentration decreases:

$$S_2O_8^{2-} + Fe^{2+} \rightarrow Fe^{3+} + SO_4^{2-} + SO_4^{\bullet -} \quad k = 15.33\,M^{-1}\,s^{-1} \tag{1}$$

$$Fe^{2+} + SO_4^{\bullet -} \rightarrow Fe^{3+} + SO_4^{2-} \quad k = 4.6 \times 10^9\,M^{-1}\,s^{-1} \tag{2}$$

However, $Fe^{3+}$ had been used as an activator for $H_2O_2$ to produce hydroxyl radicals in Fenton-like systems [17–19]. The reaction scheme shown in Eqs. (3)–(4) may explain this free radical mechanism. Because the reaction rate was slow in the $Fe^{3+}/H_2O_2$ system, an increase in the reaction temperature could enhance the system reactivity [20]:

$$Fe^{3+} + H_2O_2 \rightarrow Fe^{2+} + HO_2^{\bullet} + H^+ \tag{3}$$

$$Fe^{2+} + H_2O_2 \rightarrow Fe^{3+} + OH^- + {}^{\bullet}OH \tag{4}$$

The transformation of $Fe^{3+}$ to $Fe^{2+}$ in the $Fe^{3+}/H_2O_2$ system could be accelerated by introducing ultraviolet (UV) light via Eqs. (5)–(6) [21–24]. In addition, electrochemical technologies have been employed to promote $Fe^{2+}$ regeneration in the $Fe^{3+}/H_2O_2$ or $Fe^{2+}$/PS system [25]. Furthermore, $Fe^{2+}$ has been directly replaced by $Fe^{3+}$, which is formed in the electro/$Fe^{3+}$/persulfate process. Most of the studies with $Fe^{3+}$ have focused on its photo or electrochemical reduction to generate $Fe^{2+}$:

$$Fe(OH)^{2+} + hv \rightarrow Fe^{2+} + {}^{\bullet}OH \tag{5}$$

$$Fe(OH)_6^{3+} + hv \rightarrow Fe^{2+} + {}^{\bullet}OH + H^+ \tag{6}$$

In our study, the $Fe^{3+}$/PS system was employed to efficiently remove organic matter (i.e. Rhodamine B (RhB)) without introducing UV or electrochemical technologies, even under dark conditions. First, $Fe^{3+}$ was reduced to $Fe^{2+}$, and then, activated PS was employed to generate sulfate radicals. The effects of some important reaction parameters (i.e. PS and $Fe^{3+}$ concentrations, initial pH, and inorganic anions) on the degradation efficiencies were investigated. The mineralization of RhB was also investigated in this study. The mechanism of $Fe^{3+}$ reduction to $Fe^{2+}$ was the main part of this work.

## 2. Materials and methods

### 2.1. Materials

RhB, iron(III) nitrate monohydrate, hydrogen peroxide (30%, w/v), peroxymonosulfate, sodium nitrite, sodium sulfate, sodium nitrate, sodium chloride, and monosodium phosphate were purchased from Sinopharm Chemical Reagents (Shanghai, China). Potassium persulfate (PS) was obtained from the Aladdin Company. All of the reagents used in this study were of analytical grade. All of the solutions were prepared with doubly distilled water (DDW). In addition, the pH of the solutions was adjusted with 0.05 mol/L $HNO_3$ or NaOH.

### 2.2. Experimental

In this study, all of the RhB degradation experiments were carried out in 1 L flasks under mechanical stirring at a temperature of approximately 25℃. The time of $Fe^{3+}$ and persulfate addition was considered to be the beginning of the reaction. At scheduled time intervals, 5 mL of the solution were removed from the reactor, and then, excess $NaNO_2$ was added to the samples to consume the residual persulfate to prevent further reactions. Finally, the suspended particles were removed by centrifugation, and the supernatant was analyzed.

### 2.3. Analysis

The supernatant concentration was measured at 552 nm using UV–vis spectrophotometry (UNICO, UV-2100), and the UV–vis absorption spectra of the supernatants were also recorded. The total organic carbon (TOC) was determined using an Analyfik Jena AGN/C 2100 instrument (infra-red cell detector). The volume of the sample used for TOC analysis is 5 mL. The ferric ion concentration in solution was measured using UV–vis spectrophotometry at 665 nm.

The intermediates generated during RhB degradation were detected by GC/MC (Agilent 5775C, USA) using the following pre-treatment: the pH of the 25 mL reacted solution was adjusted to 2 with 10%

HCl, and the solution was extracted with 25 mL of dichloromethane three times. The total extract was passed through anhydrous sodium sulfate to remove any water, and the dehydrated solution was concentrated to 1 mL by rotatory evaporator. 0.5 mL of bis(trimethylsily)trifluoroacetamide (BSTFA) was added to the concentrated sample, and then, trimethylsilylation of the total solution was performed at 50℃ for 30 min. Finally, a 1 μL sample was injected into GC using the following temperature programming mode: an initial temperature of 40℃ was maintained for 4 min followed by ramping to 80℃ (10℃/min rate), which was maintained for 2 min, and ramping to 280℃ (10℃/min rate), which was maintained for 10 min.

## 3. Results and discussion

### 3.1. Catalytic mechanism of RhB degradation in the $Fe^{3+}$/PS system

Control experiments were carried out to determine RhB removal by only ferric nitrate or sulfate, and the results are presented in Fig. 1. As the reaction time increased, almost no change in the RhB concentration was observed when only $Fe^{3+}$ (from $Fe(NO_3)_3$) was added. RhB degraded gradually in the PS, $Fe^{3+}$/PS ($Fe(NO_3)_3$) or $Fe^{3+}$/PS ($Fe_2(SO_4)_3$) systems. The pHs for all control experiments had a slightly reduction trend with the extension of reaction time and the final pHs remained constant at 2.7 ± 0.2. When only PS was added to the control experiment, only 11.20% RhB degradation was observed in 60 min. The RhB degradation rate in the $Fe^{3+}$/PS ($Fe(NO_3)_3$) system (0.0583 $min^{-1}$) was slower than that in the $Fe^{3+}$/PS ($Fe_2(SO_4)_3$) system (0.0881 $min^{-1}$). When the reaction time was 30 min, the degradation efficiencies in the $Fe^{3+}$/PS ($Fe(NO_3)_3$) and $Fe^{3+}$/PS ($Fe_2(SO_4)_3$) system were 92.02 and 78.79%, respectively. Thus, $Fe(NO_3)_3$ was selected as the source of $Fe^{3+}$ in the remaining experiments.

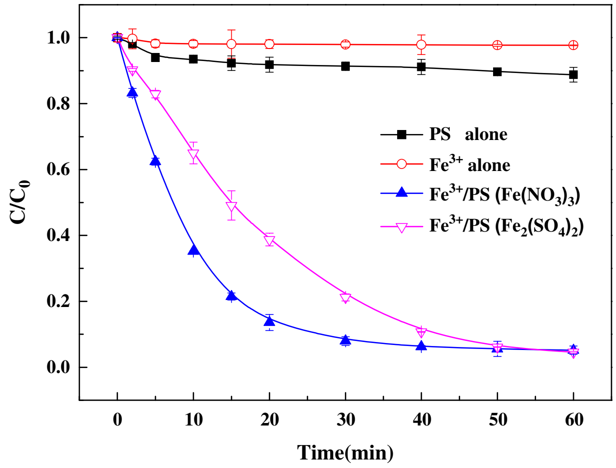

Fig. 1. Degradation of RhB under different reaction conditions. Experimental conditions: 0.052 mM $[RhB]_0$, 1 mM $[Fe^{3+}]_0$, 1 mM $[PS]_0$, $pH_{initial} = 3.0$.

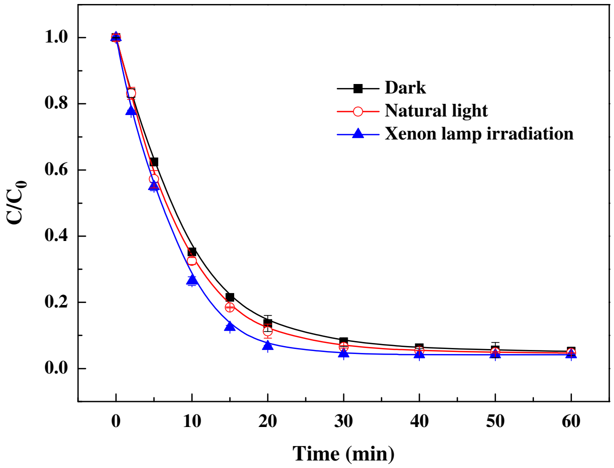

Fig. 2. Effect of different light environments on RhB degradation efficiencies. Experimental conditions: 0.052 mM $[RhB]_0$, 1 mM $[Fe^{3+}]_0$, 1 mM $[PS]_0$, $pH_{initial} = 3.0$.

The above experiments were carried out in the dark, and the $Fe^{3+}$/PS system completely removed the RhB within 60 min. In order to determine the type of radicals that had a significant influence on RhB degradation in the $Fe^{3+}$/PS system, tert-butyl alcohol (TBA, without R-hydrogen) and ethanol (EtOH, containing R-hydrogen) were chosen as scavengers for $^{\cdot}OH$ and $SO_4^{\cdot -}$ and $^{\cdot}OH$, respectively [26,27]. A molar ratio scavenger/PS of 50/1 was used in each studied system. As displayed in Fig. S1, after 60 min, the RhB degradation efficiency decreased from 100 to 92.57% with the addition of 50 mM TBA. However, the addition of 50 mM EtOH resulted in a decrease in the degradation efficiency from 100 to 18.84% as the reaction time increased. The final pHs remained constant at 2.7 ± 0.2. The loss of degradation efficiency caused by EtOH was higher than that with TBA. 73.73% RhB was degraded by the oxidation of $SO_4^{\cdot -}$. It could attribute 7.43% of $^{\cdot}OH$ responsible for RhB degradation. Therefore, $SO_4^{\cdot -}$ was predominantly produced over $^{\cdot}OH$ in the $Fe^{3+}$/PS system. In comparison to $^{\cdot}OH$, the influence of $SO_4^{\cdot -}$ on RhB degradation was more important.

In the $Fe^{3+}/H_2O_2$ system, the introduction of light sources could enhance the degradation of pollutants as the second mechanism. $Fe(OH)^{2+}$ could decompose into $Fe^{2+}$ and a hydroxide radical via Eq. (5), and the

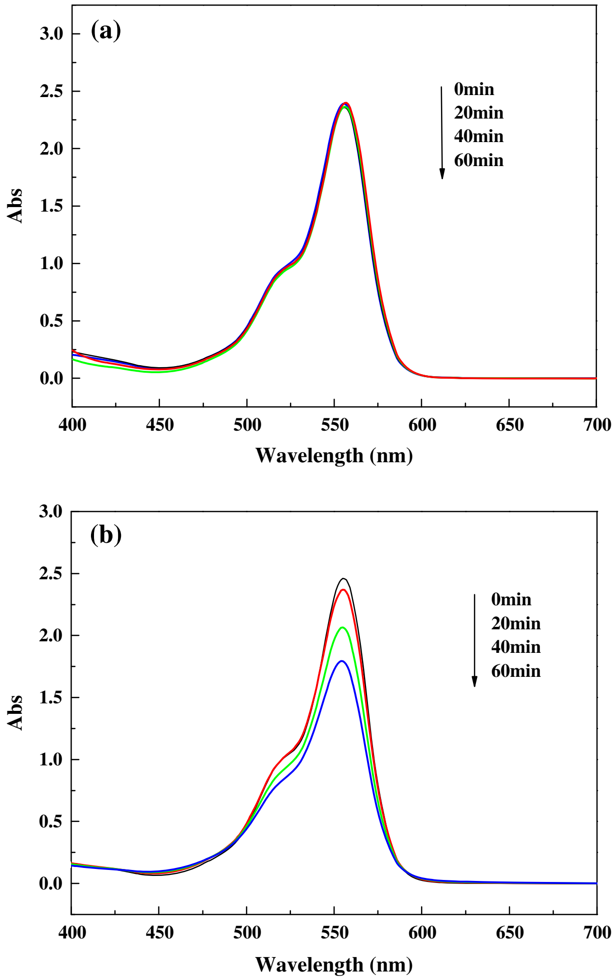

Fig. 3. UV–vis spectra of the complexation between Fe(III) and RhB: (a) dark and (b) xenon lamp irradiation. Experimental conditions: 0.052 mM $[RhB]_0$, 1 mM $[Fe^{3+}]_0$, $pH_{initial} = 3.0$.

generated $Fe^{2+}$ could be employed as an activator for $H_2O_2$ to form hydroxide radicals, which can directly oxidize pollutants. However, laser flash photolysis results have suggested that electron transfer between the excited dye and $Fe^{3+}$ involve two types of bimolecular processes as follows [22]:

$$D + Fe^{3+} \rightarrow [D\ldots Fe^{3+}] + hv \rightarrow D^{\cdot+} + Fe^{2+} \tag{7}$$

$$D + hv \rightarrow D^{*} + Fe^{3+} \rightarrow [D^{\cdot+}\ldots PFe^{3+}] \rightarrow D^{\cdot+} + Fe^{2+} \tag{8}$$

In order to confirm the electron transfer process between the excited dye and $Fe^{3+}$, a luminous experiment was introduced into the $Fe^{3+}$/PS system. Comparative experiments in the presence of $Fe^{3+}$ and PS were carried out for RhB degradation, as shown in Fig. 2. RhB decreased as the reaction time increased. The final pHs for all different light environments remained constant at 2.7 ± 0.2. Xenon lamp irradiation and natural light slightly accelerated the dye removal efficiencies compared to that in the dark. This promotion may be due to electron transfer between the excited dye and $Fe^{3+}$ based on Eqs. (7)–(8).

Fig. 3 illustrates the UV–vis spectra of RhB samples in the presence of $Fe^{3+}$ without PS under two conditions (i.e. (a) in the dark and (b) under visible light irradiation). The final pHs had a slightly reduction trend with the extension of reaction time, remained at 2.7 ± 0.2. As shown in Fig. 3(a), no loss of RhB was observed at the characteristic band with the increasing reaction time in the dark environment. However, a gradual decrease in the RhB absorbance at 552 nm was found under visible light irradiation (Fig. 3(b)). Due to conversion into other substances, RhB was reduced under visible light. This phenomenon demonstrated that RhB became the excited dye under visible light irradiation and then formed complexes with $Fe^{3+}$ Eq. (8) rather than reacting with $Fe^{3+}$ to directly generate complexes Eq. (7).

However, RhB can be effectively removed in the presence of $Fe^{3+}$ and persulfate in the dark environment. This phenomenon may be due to RhB being oxidized by persulfate to generate organic intermediates (Fig. 1), and these intermediates acted as electron transfer agents to reduce $Fe^{3+}$ to $Fe^{2+}$ [28]. In order to confirm the existence of the organic intermediates, the UV–vis spectra of RhB degradation using only persulfate is demonstrated in Fig. S2. The final pH for the experiments had a slightly reduction trend with the extension of reaction time and remained constant at 2.7 ± 0.2. The absorbance strength increased compared to the control sample in a range from 350 to 500 nm, which may be due to the formation of quinone compounds in this system [29]. Quinone compounds, such as hydroqinone and benzoquinone, can reduce $Fe^{3+}$ to $Fe^{2+}$ at a low pH [30]. And, the generated $Fe^{2+}$ could react with persulfate to generate sulfate radicals, which can initiate RhB degradation.

Fig. S3 shows the UV–vis spectra for RhB degradation in the $Fe^{3+}$/PS system. It was found that the reaction time was longer, the higher absorbance intensity was gained in the range of 350–500 nm. Such a behavior may be due to the generation of numerous intermediates including quinone compounds resulting from attacks by the sulfate radicals in the $Fe^{3+}$/PS system, which resulted in $Fe^{3+}$ reduction and $Fe^{2+}$ regeneration by generated organic intermediates in the RhB degradation system.

In addition, Minisci et al. [31] indicated that organic compounds might surrender to the organic

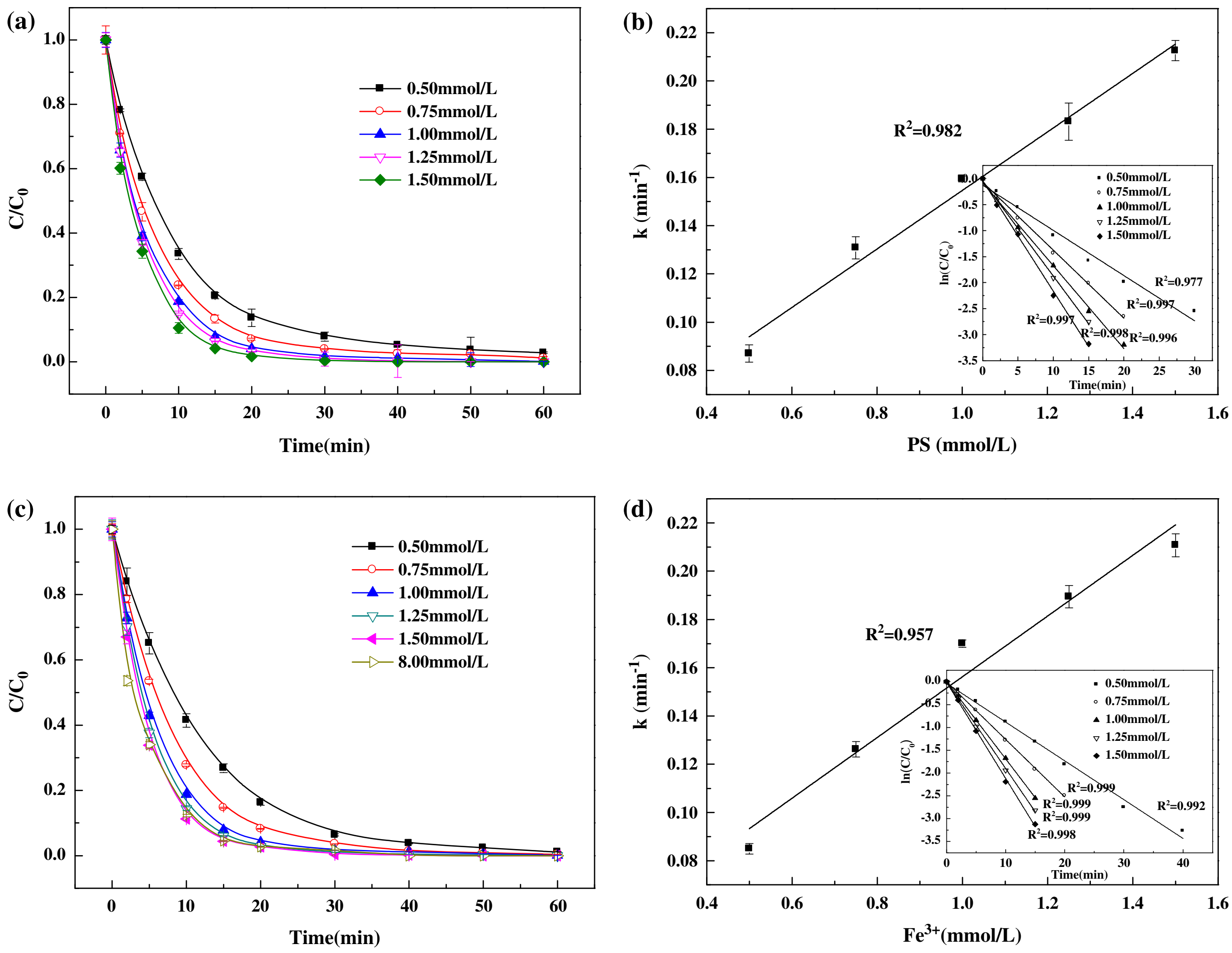

Fig. 4. Effects of (a and b) PS and (c and d) $Fe^{3+}$ concentration on RhB degradation. Experimental conditions: 0.052 mM $[RhB]_0$, $pH_{initial} = 3.0$, 1 mM $[Fe^{3+}]_0$ (a and b), 1 mM $[PS]_0$ (c and d).

radicals via oxidation of $SO_4^{\cdot-}$ during the degradation process. Organic radicals could promote the transformation of $Fe^{3+}$ to $Fe^{2+}$. Therefore, $SO_4^{\cdot-}$, which was formed by the $Fe^{3+}$/persulfate system, could completely remove RhB when $Fe^{2+}$ was continuously produced from $Fe^{3+}$ due to the reduction of the intermediates.

### 3.2. Effects of the PS and $Fe^{3+}$ concentrations on RhB degradation

The PS concentration plays an important role as the source of sulfate radicals in the $Fe^{3+}$/PS system. In order to analyze the effect of the PS dosage on RhB degradation, the experiments were carried out by varying the PS concentration from 0.5 to 1.5 mM with the $Fe^{3+}$ concentration held constant at 1.00 mM. Fig. 4(a) shows that with an increase in time, the RhB degradation increases. When the PS concentration varied from 0.5 to 1 mM, the RhB degradation efficiencies increased from 79.44 to 92.18% within 15 min and reached nearly 100% when the PS concentration exceeded 1 mM, and the color of the RhB solution completely faded. The final pHs for the experiments had a slightly reduction trend with the increase of reaction time and remained at 2.7 ± 0.5. RhB degradation follows first-order kinetics. The reaction rate constant (*k*) increased significantly with the PS dosage from 0.087 to 0.212 $min^{-1}$ when the PS concentration increased from 0.5 to 1.5 mM (Fig. 4(b)). This result was due to the higher sulfate concentration resulting in a larger number of sulfate radicals being produced per unit time, which resulted in faster RhB degradation. However, a further increase in the PS

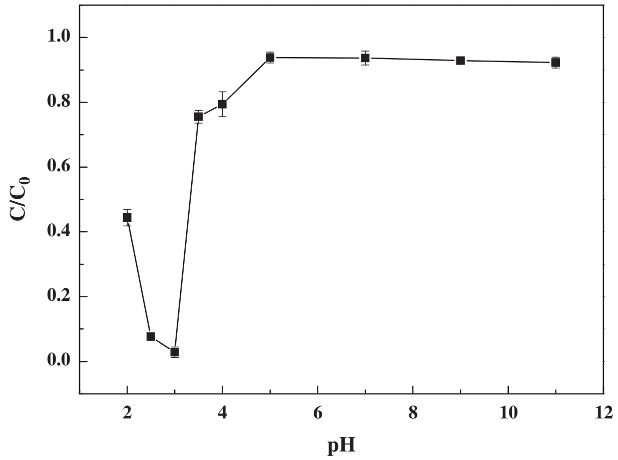

Fig. 5. Effect of initial pH on RhB degradation efficiencies in 60 min. Experimental conditions: 0.052 mM $[RhB]_0$, 1 mM $[Fe^{3+}]_0$, 1 mM $[PS]_0$.

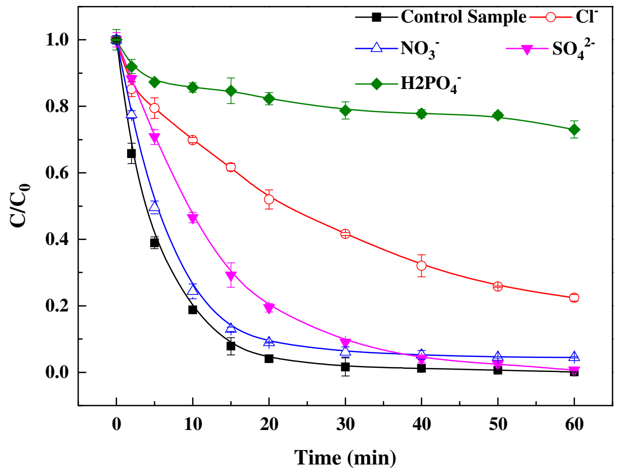

Fig. 6. Effect of different inorganic salts on RhB degradation efficiencies. Experimental conditions: 0.052 mM $[RhB]_0$, 1 mM $[Fe^{3+}]_0$, 1 mM $[PS]_0$, 1 mM $[anion]_0$, $pH_{initial}$ = 3.0.

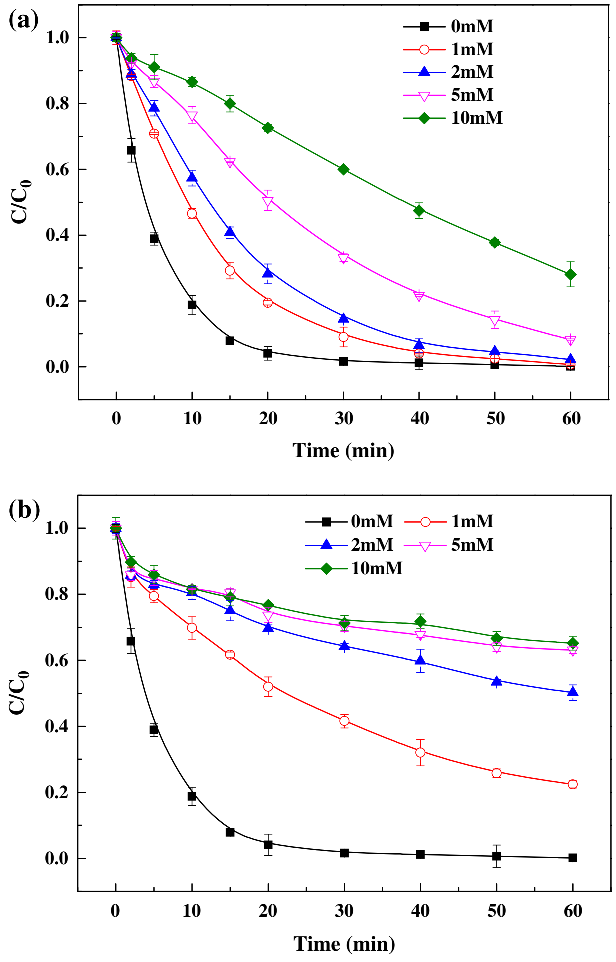

Fig. 7. Effects of different $SO_4^{2-}$ (a) and $Cl^-$ (b) concentrations on RhB degradation efficiencies. Experimental conditions: 0.052 mM $[RhB]_0$, 1 mM $[Fe^{3+}]_0$, 1 mM $[PS]_0$, $pH_{initial}$ = 3.0.

concentration to more than 1 mM only resulted in a slight increase in RhB removal because this concentration was sufficiently high for the $Fe^{3+}$ load when the PS concentration reached a certain value.

Because $Fe^{3+}$ was reduced to $Fe^{2+}$ to catalyze persulfate, the production sulfate radicals from persulfate, its existence could significantly affect the pollutant degradation efficiency. The effect of different $Fe^{3+}$ concentrations on the RhB degradation efficiency is displayed in Fig. 4(c). The amount of RhB decreased with the extension of reaction time. As the $Fe^{3+}$ initial concentration increased, the RhB degradation increased. The final pHs for the experiments remained at 2.7 ± 0.2. As mentioned above, $Fe^{2+}$ could be used as a sulfate radical scavenger at high concentrations, and the results shown in Fig. 4(c) indicated that an increase in the $Fe^{3+}$ concentration to 8 mM accelerated RhB degradation, which could reach 46.39% within 2 min, rather than reducing the degradation efficiency. The higher $Fe^{2+}$ concentration was due to the reduction of $Fe^{3+}$, which could improve the decomposition rate of persulfate to afford more sulfate radicals for RhB degradation.

The increase in RhB degradation due to an increase in the $Fe^{3+}$ content in this system was not substantial and was only reflected in the reaction rate (i.e. 0.085 $min^{-1}$ up to 0.211 $min^{-1}$ when the $Fe^{3+}$ concentration increased from 0.5 to 1.5 mM) (Fig. 4(d)).

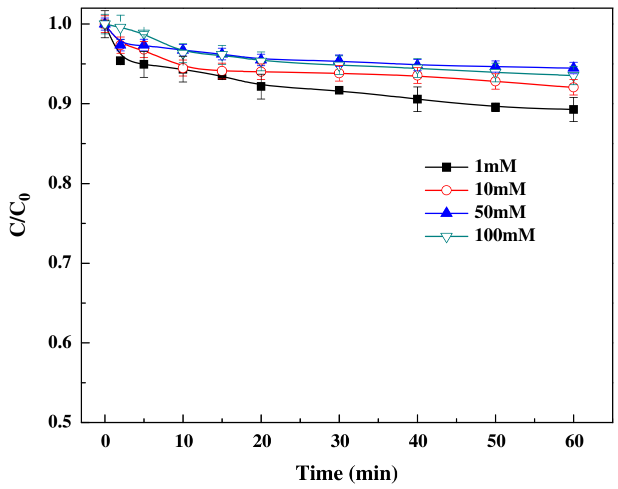

Fig. 8. RhB degradation efficiencies in the PS/Cl$^-$ system. Experimental conditions: 0.052 mM $[\mathrm{RhB}]_0$, 1 mM $[\mathrm{Fe}^{3+}]_0$, 1 mM $[\mathrm{PS}]_0$, $\mathrm{pH}_{\mathrm{initial}} = 3.0$.

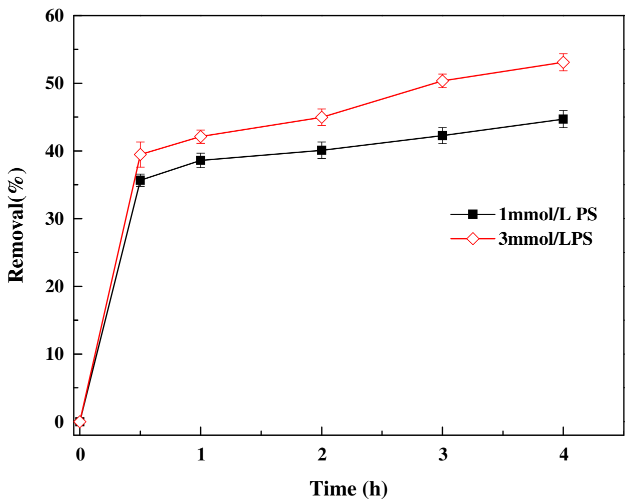

Fig. 9. TOC removal efficiencies of the RhB solution under different PS concentrations. Experimental conditions: 0.052 mM $[\mathrm{RhB}]_0$, 1 mM $[\mathrm{Fe}^{3+}]_0$, $\mathrm{pH}_{\mathrm{initial}} = 3.0$.

### 3.3. Effect of initial pH

The effect of the initial pH on the RhB degradation efficiencies in 60 min was explored in an extensive pH range from 2 to 11, and the results are illustrated in Fig. 5. These results demonstrated that the RhB degradation efficiencies directly depended on the initial pH. With the increase of pH from 2 to 3, the degradation efficiency of RhB changed from 55.60 to 98.18%. The optimal RhB degradation efficiency was observed at an initial pH of approximately 3.0. The final pH after accomplishment of the reaction after 60 min of reaction timer remained at 2.7 ± 0.2. The RhB degradation efficiency decreased with increasing pH. At a pH of 11, the RhB degradation efficiency was only 7.71%. Due to the hydrolysis of solution $\mathrm{Fe}^{3+}$, the solution pH decreased sharply from 3.80 to 3.06, and no pH adjustment occurred in this system. The changed in pH (approximately –0.06) due to persulfate addition was neglected.

The decrease in RhB degradation in the lower pH range (pH < 3.0) was primarily due to the formation of $\mathrm{Fe}^{2+}$ complexes Eq. (9) through the generated $\mathrm{Fe}^{2+}$ [32], which could hinder further reaction of $\mathrm{Fe}^{2+}$ and persulfate. Another possible reason might be that the formation of sulfate radical could be accelerated by the decomposition of persulfate at lower pH values Eqs. (10)–(11) [33], and the generated abundant sulfate radicals could not be transferred to the surface of the organic compound for degradation in time and were consumed by themselves (Eq. (12)) or reacted with PS to form $\mathrm{SO}_4^{2-}$ (Eq. (13)) [34,35]:

$$\mathrm{Fe}^{2+} + \mathrm{H_2O} \rightarrow [\mathrm{Fe(H_2O)}]^{2+} \tag{9}$$

$$\mathrm{H}^+ + \mathrm{S_2O_8^{2-}} \rightarrow \mathrm{HS_2O_8^-} \tag{10}$$

$$\mathrm{HS_2O_8^-} \rightarrow \mathrm{H}^+ + \mathrm{SO_4^{\cdot -}} + \mathrm{SO_4^{2-}} \tag{11}$$

$$\mathrm{SO_4^{\cdot -}} + \mathrm{SO_4^{\cdot -}} \rightarrow \mathrm{S_2O_8^{2-}} \tag{12}$$

$$\mathrm{SO_4^{\cdot -}} + \mathrm{S_2O_8^{2-}} \rightarrow \mathrm{S_2O_8^{\cdot -}} + \mathrm{SO_4^{2-}} \tag{13}$$

However, the RhB efficiencies decreased rapidly when the initial pH was increased to a higher pH level. For example, the RhB degradation efficiency was only 22.46% when the initial pH was increased to 3.5. More $\mathrm{Fe}^{3+}$ and $\mathrm{Fe}^{2+}$ hydroxide complexes, such as $\mathrm{Fe(OH)}_3^0$, $\mathrm{FeOH}^{2+}$, $\mathrm{Fe(OH)}^{2+}$, and $\mathrm{Fe_2(OH)}_2^{4+}$, could be produced as the initial pH increased [36], and these complexes had a lower activation capacity for persulfate and a negative impact on the generation of sulfate radicals. Another study on RhB degradation by the $\mathrm{Fe}^{2+}$/oxone system confirmed that a higher degradation efficiency could be achieved under acidic pH conditions [37]. Consequently, an optimal initial pH of 3.0 without any adjustment is recommended for RhB degradation.

### 3.4. Effect of various inorganic ions

Usually, a large amount of salts are employed in various dyeing processes. Previous studies have reported that the presence of some inorganic ions can affect the degradation of organic compounds in SR-AOPs. The presence of NaCl, $\mathrm{Na_2SO_4}$, and $\mathrm{NaNO_3}$

exhibited improved, retarded, and null effects, respectively, on the RhB degradation in a $Fe^{2+}$/oxone system [37]. In addition, $Cl^-$ and $H_2PO_4^-$ had a noticeably negative effect on carbamazepine degradation in the $Fe^{2+}$/PS system [38]. In this study, the RhB degradation performance using four different inorganic ions (i.e. NaCl, $Na_2SO_4$, $NaNO_3$, and $NaH_2PO_4$) was evaluated by comparison to a control sample.

As shown in Fig. 6, the RhB concentration declined with increasing reaction time. The final pHs after accomplishments of the reactions after 60 min of reaction timer remained at 2.7 ± 0.2. The addition of 1 mM $H_2PO_4^-$ obviously inhibited RhB degradation, which was similar to the $Fe^{2+}$/PS process for orange G degradation [39]. Due to the complex formation ($H_2PO_4^-$-Fe) between $H_2PO_4^-$ and iron in aqueous media, the free $Fe^{2+}$ in the solution which could react with the persulfate reduced [11,38]. Because $NO_3^-$ does not form complexes with iron, it is an invalid scavenger for sulfate radicals. $NO_3^-$ showed an insignificant effect on RhB degradation. The feeble negative effect mainly caused by the high ion strength after $NO_3^-$ addition leads to a slower decomposition of persulfate [40].

The RhB degradation efficiency decreased after the addition of $SO_4^{2-}$. To investigate the effect of $Na_2SO_4$ on RhB removal, the experiments were performed by varying the $SO_4^{2-}$ concentration from 0.0 to 10 mM, and the results are demonstrated in Fig. 7(a). With the extension of time, the amount of RhB and the final pHs gradually decreased. And with the increase of $SO_4^{2-}$ concentration, the RhB degradation also decreased. The final pHs were 2.7 ± 0.2.

This result may be due to the increase in $SO_4^{2-}$ leading to a decrease in the rate of persulfate decomposition resulting from complexation reactions between iron and $SO_4^{2-}$ [41]. For example, based on the visual MINTEQ calculation, the formation of the Fe-$SO_4^{2-}$ complex could consume approximately 74% of the initiate 1 mM $Fe^{3+}$ at pH 3.0 with the addition of 5 mM $SO_4^{2-}$. Because of the lower activation efficiency of these complexes for persulfate, the formation of sulfate radicals decreased, and the RhB degradation efficiency declined. Moreover, the addition of $SO_4^{2-}$ could reduce the half-reaction reduction potential of the sulfate radicals according to Eq. (14).

$$E_{(SO_4^{\bullet-}/SO_4^{2-})} = E^{\theta}_{(SO_4^{\bullet-}/SO_4^{2-})} + \frac{RT}{zF}\ln\frac{[SO_4^{\bullet-}]}{[SO_4^{2-}]} \tag{14}$$

where $E_{(SO_4^{\bullet-}/SO_4^{2-})}$ is the half-reaction reduction potential, $E^{\theta}_{(SO_4^{\bullet-}/SO_4^{2-})}$ is the standard half-reaction reduction potential, $R$ is the universal gas constant (8.314472 $JK^{-1}\ mol^{-1}$), $T$ is the absolute temperature, $F$ is the Faraday constant ($9.6485 \times 104\ Cmol^{-1}$), and $z$ is the number of electrons transferred in the half-reaction. According to Eq. (14), the redox potential of $SO_4^{\bullet-}/SO_4^{2-}$ was affected by the concentration of $SO_4^{2-}$.

The negative effect of $Cl^-$ on RhB degradation was found in Fig. 7(b). The RhB concentration reduced with the extension of reaction time. The RhB degradation efficiencies were repressive as the increase of $Cl^-$ concentration. And the final pHs remained at 2.7 ± 0.2. It is important to note that this result was entirely different from that observed with the $Fe^{2+}$/oxone system for RhB degradation, which was accelerated after $Cl^-$ addition [37]. In their study, the RhB degradation was due to the co-existence of PMS and chloride without $Fe^{2+}$ because the generation of HOCl occurred via Eq. (15). It indicated that HOCl possessed sufficient oxidation ability for RhB degradation. Based on the thermodynamics, $S_2O_8^{2-}$ ($E^0 = 2.01$ V) could oxidize $Cl^-$ to form chlorine ($Cl_2/Cl^-$, 1.36 V) and hypochlorous acid ($HOCl/Cl^-$, 1.48 V).

$$HSO_5^- + Cl^- \rightarrow SO_4^{2-} + HOCl \tag{15}$$

As shown in Fig. 8, the RhB concentration was nearly unchanged in the PS/$Cl^-$ system when the reaction time was extended to 60 min. With the increase of $Cl^-$ concentration, RhB degradation decreased. And the final pHs remained at 2.7 ± 0.2. The results indicated that $Cl_2$ and HOCl were not formed in the PS/$Cl^-$ system. Bennedsen et al. [42] reported that PCE degradation and persulfate consumption decreased exponentially as the $Cl^-$ concentration increased. The presence of $Cl^-$ did not affect sulfate radicals as scavengers but affected the formation of sulfate radicals by complexation with iron.

### *3.5. Mineralization of RhB*

Although RhB degradation in the $Fe^{3+}$/PS system could occur quickly in 60 min, the TOC removal efficiency of the RhB solution was much slower than the RhB degradation efficiency. Fig. 9 displays the TOC removal of the RhB solution under different PS concentrations. The results indicated that the TOC removal efficiencies were positively associated with the persulfate concentration. The removal of TOC increased with the extension of reaction time, and the removal of TOC improved in a PS concentration range of 1–3 mM. TOC reduction in the RhB solution was very similar at PS concentration of 1 and 3 mM with a TOC removal of 35.68 and 39.47%, respectively, in 30 min.

At the beginning of the degradation reaction, the PS concentration was sufficient to generate sulfate radicals at a fixed $Fe^{3+}$ dosage. When the reaction lasted 4 h with the constant consumption of PS, the TOC removal efficiencies varied for the systems with PS concentrations of 1 and 3 mM (i.e. 44.70 and 53.09%, respectively). Therefore, a higher concentration of PS could enhance RhB degradation by providing more sulfate radicals.

The reaction intermediates generated in RhB degradation by the $Fe^{3+}$/PS system are listed in Table S1. Fig. S4 shows the GC/MS chromatogram of these intermediates. The reaction intermediates primarily consisted of acids and alcohols in the final reaction liquid (60 min) (i.e. 2-hydroxy propionate, phenylacetic acid, 2-phenyl-2-propanol, glycerol, 4-methyl-1,2-butyl glycol, acetophenone, and dibutyl phthalate).

## 4. Conclusions

RhB was successfully removed from aqueous solutions using the $Fe^{3+}$/PS system. The possible reaction mechanism involved the generation of intermediate products during RhB degradation, which could act as electron transmitters to accelerate the reduction of $Fe^{3+}$ to $Fe^{2+}$ and afford complete RhB degradation. The experimental results revealed that the dye degradation efficiencies were substantially influenced by the experiment parameters, such as the $Fe^{3+}$ and persulfate concentrations, initial pH, and inorganic salts. Hundred percentage of the RhB was removed at an initial concentration of 0.052 mM in 30 min under the following conditions: 1 mM $[Fe^{3+}]_0$, 1 mM $[PS]_0$ and $pH_{initial} = 3.0$. The results indicated that higher $Fe^{3+}$ and persulfate concentrations resulted in faster degradation efficiencies. The presence of inorganic ions exhibited negative effects on RhB degradation in the following sequence: $NO_3^- < SO_4^{2-} < Cl^- < H_2PO_4^-$.

## Supplementary material

The supplementary material for this paper is available online at http://10.1080/19443994.2016.1148641.

## Acknowledgments

The authors appreciate technical support from the Instrumental Analysis & Research Center of Shanghai University. This study was financially supported by the National Nature Science Foundation of China (Nos. 41472312/D0218, 21107067/B070303) and the Innovative Research Team in University (No. IRT13078).

## References

[1] A. Asghar, A.A.A. Raman, W.M.A.W. Daud, Advanced oxidation processes for in-situ production of hydrogen peroxide/hydroxyl radical for textile wastewater treatment: A review, J. Cleaner Prod. 87 (2015) 826–838.

[2] S.W. da Silva, C.R. Klauck, M.A. Siqueira, A.M. Bernardes, Degradation of the commercial surfactant nonylphenol ethoxylate by advanced oxidation processes, J. Hazard. Mater. 282 (2015) 241–248.

[3] C.J. Li, J. Ma, J.M. Shen, P. Wang, Removal of phosphate from secondary effluent with $Fe^{2+}$ enhanced by $H_2O_2$ at nature pH/neutral pH, J. Hazard. Mater. 166 (2009) 891–896.

[4] M. Taghdiri, N. Saadatjou, N. Zamani, R. Farrokhi, Heterogeneous degradation of precipitated hexamine from wastewater by catalytic function of silicotungstic acid in the presence of $H_2O_2$ and $H_2O_2/Fe^{2+}$, J. Hazard. Mater. 246–247 (2013) 206–212.

[5] G.P. Anipsitakis, D.D. Dionysiou, Degradation of organic contaminants in water with sulfate radicals generated by the conjunction of peroxymonosulfate with cobalt, Environ. Sci. Technol. 37(20) (2003) 4790–4797.

[6] K. Govindan, M. Raja, M. Noel, E.J. James, Degradation of pentachlorophenol by hydroxyl radicals and sulfate radicals using electrochemical activation of peroxomonosulfate, peroxodisulfate and hydrogen peroxide, J. Hazard. Mater. 272 (2014) 42–51.

[7] P.C. Xie, J. Ma, W. Liu, J. Zou, S.Y.C. Yue, X. Li, M.R. Wiesner, J.Y. Fang, Removal of 2-MIB and geosmin using UV/persulfate: Contributions of hydroxyl and sulfate radicals, Water Res. 69 (2015) 223–233.

[8] M.H. Xu, X.G. Gu, S.G. Lu, Z.F. Qiu, Q. Sui, Z.W. Miao, X.K. Zang, X.L. Wu, Degradation of carbon tetrachloride in aqueous solution in the thermally activated persulfate system, J. Hazard. Mater. 286 (2015) 7–14.

[9] S.L. Wang, N. Zhou, S. Wu, Q. Zhang, Z. Yang, Modeling the oxidation kinetics of sono-activated persulfate's process on the degradation of humic acid, Ultrason. Sonochem. 23 (2015) 128–134.

[10] Y.S. Zhao, C. Sun, J.Q. Sun, R. Zhou, Kinetic modeling and efficiency of sulfate radical-based oxidation to remove p-nitroaniline from wastewater by persulfate/$Fe_3O_4$ nanoparticles process, Sep. Purif. Technol. 142 (2015) 182–188.

[11] A. Ghauch, G. Ayoub, S. Naim, Degradation of sulfamethoxazole by persulfate assisted micrometric $Fe^0$ in aqueous solution, Chem. Eng. J. 228 (2013) 1168–1181.

[12] G. Ayoub, A. Ghauch, Assessment of bimetallic and trimetallic iron-based systems for persulfate activation: Application to sulfamethoxazole degradation, Chem. Eng. J. 256 (2014) 280–292.

[13] S. Naim, A. Ghauch, Ranitidine abatement in chemically activated persulfate systems: Assessment of industrial iron waste for sustainable applications, Chem. Eng. J. 288 (2016) 276–288.

[14] S.Y. Oh, H.W. Kim, J.M. Park, H.S. Park, C. Yoon, Oxidation of polyvinyl alcohol by persulfate activated with heat, $Fe^{2+}$, and zero-valent iron, J. Hazard. Mater. 168 (2009) 346–351.

[15] H. Kusic, I. Peternel, S. Ukic, N. Koprivanac, T. Bolanca, S. Papic, A.L. Bozic, Modeling of iron activated persulfate oxidation treating reactive azo dye in water matrix, Chem. Eng. J. 172(1) (2011) 109–121.

[16] A. Ghauch, A. Tuqan, Oxidation of bisoprolol in heated persulfate/$H_2O$ systems: Kinetics and products, Chem. Eng. J. 183 (2012) 162–171.

[17] Y. Mino, Y. Moriyama, Y. Nakatake, Degradation of 2,7-dichlorodibenzo-*p*-dioxin by $Fe^{3+}$-$H_2O_2$ mixed reagent, Chemosphere 57(5) (2004) 365–372.

[18] B. McAteer, N. Beattie, D.T. Richens, Catalytic oxidation of cyclohexene by aqueous iron(III)/$H_2O_2$ in mildly acidic solution: Epoxidation versus allylic oxidation, Inorg. Chem. Commun. 35 (2013) 284–289.

[19] I. Velo-Gala, J.J. López-Peñalver, M. Sánchez-Polo, J. Rivera-Utrilla, Comparative study of oxidative degradation of sodium diatrizoate in aqueous solution by $H_2O_2/Fe^{2+}$, $H_2O_2/Fe^{3+}$, Fe(VI) and UV, $H_2O_2$/UV, $K_2S_2O_8$/UV, Chem. Eng. J. 241 (2014) 504–512.

[20] Y. Lee, C. Lee, J. Yoon, High temperature dependence of 2,4-dichlorophenoxyacetic acid degradation by $Fe^{3+}/H_2O_2$ system, Chemosphere 51(9) (2003) 963–971.

[21] Y.D. Xie, F. Chen, J.J. He, J.C. Zhao, H. Wang, Photoassisted degradation of dyes in the presence of $Fe^{3+}$ and $H_2O_2$ under visible irradiation, J. Photochem. Photobiol. A: Chem. 136(3) (2000) 235–240.

[22] F. Herrera, J. Kiwi, A. Lopez, V. Nadtochenko, Photochemical decoloration of remazol brilliant blue and uniblue a in the presence of $Fe^{3+}$ and $H_2O_2$, Environ. Sci. Technol. 33(18) (1999) 3145–3151.

[23] X.M. Li, T.T. Shen, D.B. Wang, X. Yue, X. Liu, Q. Yang, J.B. Cao, W. Zheng, G.M. Zeng, Photodegradation of amoxicillin by catalyzed $Fe^{3+}/H_2O_2$ process, J. Environ. Sci. 24(2) (2012) 269–275.

[24] C.S. Chiou, Y.H. Chen, C.T. Chang, C.Y. Chang, J.L. Shie, Y.S. Li, Photochemical mineralization of di-n-butyl phthalate with $H_2O_2/Fe^{3+}$, J. Hazard. Mater. 135(1–3) (2006) 344–349.

[25] I. Sirés, J.A. Garrido, R.M. Rodríguez, E. Brillas, N. Oturan, M.A. Oturan, Catalytic behavior of the $Fe^{3+}/Fe^{2+}$ system in the electro-Fenton degradation of the antimicrobial chlorophene, Appl. Catal. B: Environ. 72 (3–4) (2007) 382–394.

[26] G.V. Buxton, C.L. Greenstock, W.P. Helman, A.B. Ross, Critical review of rate constants for reactions of hydrated electrons, hydrogen atoms and hydroxyl radicals ($^{\bullet}OH/^{\bullet}O^{-}$) in aqueous solution, J. Phys. Chem. Ref. Data 17(2) (1988) 513–886.

[27] P. Neta, J. Grodkowski, A.B. Ross, Rate constants for reactions of aliphatic carbon-centered radicals in aqueous solution, J. Phys. Chem. Ref. Data 25(3) (1996) 709–1050.

[28] S. Rodriguez, L. Vasquez, D. Costa, A. Romero, A. Santos, Oxidation of Orange G by persulfate activated by Fe(II), Fe(III) and zero valent iron (ZVI), Chemosphere 101 (2014) 86–92.

[29] A. Aguiar, A. Ferraz, $Fe^{3+}$- and $Cu^{2+}$-reduction by phenol derivatives associated with Azure B degradation in Fenton-like reactions, Chemosphere 66(5) (2007) 947–954.

[30] R.Z. Chen, J.J. Pignatello, Role of quinone intermediates as electron shuttles in fenton and photoassisted fenton oxidations of aromatic compounds, Environ. Sci. Technol. 31(8) (1997) 2399–2406.

[31] F. Minisci, A. Citterio, Electron-transfer processes: Peroxydisulfate, a useful and versatile reagent in organic chemistry, Acc. Chem. Res. 16 (1983) 27–32.

[32] N. Masomboon, C. Ratanatamskul, M.C. Lu, Chemical oxidation of 2,6-dimethylaniline in the Fenton process, Environ. Sci. Technol. 43(22) (2009) 8629–8634.

[33] C.J. Liang, C.F. Huang, Y.J. Chen, Potential for activated persulfate degradation of BTEX contamination, Water Res. 42(15) (2008) 4091–4100.

[34] X.Y. Yu, Z.C. Bao, J.R. Barker, Free radical reactions involving $Cl^{\bullet}$, $Cl_2^{-\bullet}$, and $SO_4^{-\bullet}$ in the 248 nm photolysis of aqueous solutions containing $S_2O_8^{2-}$ and $Cl^{-}$, J. Phys. Chem. A 108 (2004) 295–308.

[35] G.P. Anipsitakis, D.D. Dionysiou, Radical generation by the interaction of transition metals with common oxidants, Environ. Sci. Technol. 38(13) (2004) 3705–3712.

[36] A. Stefánsson, Iron(III) Hydrolysis and Solubility at 25˚C, Environ. Sci. Technol. 41(17) (2007) 6117–6123.

[37] Y.R. Wang, W. Chu, Degradation of a xanthene dye by Fe(II)-mediated activation of Oxone process, J. Hazard. Mater. 186(2–3) (2011) 1455–1461.

[38] Y.F. Rao, L. Qu, H.S. Yang, W. Chu, Degradation of carbamazepine by Fe(II)-activated persulfate process, J. Hazard. Mater. 268 (2014) 23–32.

[39] X.R. Xu, X.Z. Li, Degradation of azo dye Orange G in aqueous solutions by persulfate with ferrous ion, Sep. Purif. Technol. 72(1) (2010) 105–111.

[40] K.C. Huang, R.A. Couttenye, G.E. Hoag, Kinetics of heat-assisted persulfate oxidation of methyl tert-butyl ether (MTBE), Chemosphere 49(4) (2002) 413–420.

[41] J. De Laat, G.T. Le, B. Legube, A comparative study of the effects of chloride, sulfate and nitrate ions on the rates of decomposition of $H_2O_2$ and organic compounds by Fe(II)/$H_2O_2$ and Fe(III)/$H_2O_2$, Chemosphere 55(5) (2004) 715–723.

[42] L.R. Bennedsen, J. Muff, E.G. Søgaard, Influence of chloride and carbonates on the reactivity of activated persulfate, Chemosphere 86(11) (2012) 1092–1097.